Influence of heat input and powder density on energetic efficiency of high power diode laser cladding of carbon steel with AISI316L powder

S. Zanzarin, S. Bengtsson, L. Maines, A. Molinari

High power diode laser with coaxial powder injection was used to deposit single tracks of austenitic stainless steel on to a carbon steel plate, and the influence of heat input and powder density on energetic efficiency of the process, as well as on some geometrical features of the clad and on dilution was investigated. The energetic efficiency, calculated as the energy used to form the clad and the Heat Affected Zone, tends to increase with the powder density, while it decreases on increasing heat input. The combination of a high powder density and a low heat input is expected to optimize the energetic efficiency. In these conditions, the chemical dilution of the clad is minimized whilst aspect ratio is rather low but still acceptable. Moreover, the energy spent for the powder and the substrate can be correlated to the iron contamination of the clad.

Keywords: Laser cladding - Powder density - Heat input - Energetic efficiency

INTRODUCTION

Laser cladding is a surface coating technology where a powder or a wire is melted and consolidated on a substrate using a laser beam as a heat source. This technique allows the production of full-dense and crack-free coatings, with an excellent metallurgical bond and a low dilution, i.e. a low contamination by the substrate material. The thickness of the clad ranges typically from 0.5 to 2 mm [1-4].
The coating material may be delivered to the cladding system in three different ways: a wire is fed directly into the melt pool; a powder is preplaced on a substrate; a powder is injected into the melt pool either laterally or coaxially to the laser beam [1-3]. Among these techniques, the coaxial laser cladding method has several advantages: velocity (one-step process), a better control of dilution, the

Simone Zanzarin, Lorena Maines, Alberto Molinari

Department of Industrial Engineering
University of Trento
Trento, Italy

Sven Bengtsson

Höganäs AB, Höganäs, Sweden

Corresponding author: Simone Zanzarin

Department of Industrial Engineering University of Trento (Italy), Via Mesiano 77 - 38123 Trento

Tel. +39 (0)461 282402, Fax +39 (0)461 281977, E-mail: simone.zanzarin@unitn.it

adaptability on complex geometrical shapes and the independency on the cladding direction [3].
The main parameters of laser cladding are the laser power, the scan speed and the powder feed rate, even if several other parameters related to powder, laser beam, shield and carrier gases and geometry of the system are also important [3, 5-7].
In the present work the results of an investigation of a single track laser cladding of a carbon steel plate with austenitic stainless steel powders are presented. A coaxial high power diode laser was used and the laser power, the scan speed and the powder feed rate were varied to investigate their effect on the energetic efficiency of the process. The energy delivered by the laser is split in two main portions: that spent to form the clad, by melting and overheating the powder and the substrate, and the heat affected zone and that lost by the contribution of several dissipative phenomena [8, 9]. In principle the high power diode laser is characterized by a higher energy efficiency in comparison to other lasers [10, 11], but efficiency may depend on the processing parameters.

EXPERIMENTAL PROCEDURE

The powder used is water atomized AISI 316L (17.1% Cr, 11.7% Ni, 2.4% Mo, 1.6% Mn, 1,6% Si, 0.017% C). Six different clads were produced on a carbon steel substrate, by using a Coherent HighLight 4000L high power diode laser with coaxial feeding of the stainless steel powder. The laser spot is 12 mm wide and 1 mm long. The processing conditions for the six clads are reported in Table I: in addition to the power P, the scan speed v and the feed rate f, the heat

input H_{in} (=P/v) and the powder density G ($G=f/vD$ where D is the main dimension of the laser beam), are reported. These two parameters are indeed frequently used to describe the process [1, 2, 12-14], due to the importance of the interactions between the single variables.

clad	Power (kW)	Scan speed (mm/s)	Feed rate (g/s)	Heat input (J/mm)	Powder density (g/mm²)
1	3.0	6.0	0.464	500	0.0064
2	3.0	4.0	0.464	750	0.0097
3	3.0	4.0	0.663	750	0.0138
4	2.0	4.0	0.295	500	0.0062
5	2.0	4.0	0.464	500	0.0097
6	4.0	4.0	0.464	1000	0.0097

Table I - Cladding parameters of the six samples

Tabella I - Parametri di processo dei sei campioni

The macrostructure of the six clads along the transversal direction is shown in Figure 1 in a powder density / heat input diagram: no pores and cracks are observed.
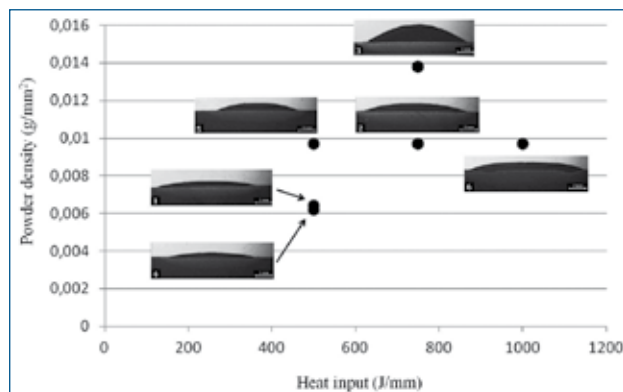
Fig. 1 - Macrostructure of the clads

Fig. 1- Macrostruttura dei campioni

The microstructure is not influenced by the processing parameters significantly; Figure 2 shows, as an example, the cellular solidification structure of the clad (2a), the microstructure at the interface (2b) and the coarse bainitic (close to interface) and pearlitic/ferritic microstructure (close to unaffected substrate) of Heat Affected Zone (HAZ) (2c and 2d) in clad 3. Etching was made either with 2% Nital, to highlight the microstructure of HAZ, or electrolitically in an aqueous solution of oxalic acid (9% in weight), applying a potential of 4 V for a time of 4-20 s.
The powder lost during cladding was measured by weighing the substrate plate before and after cladding using a balance with a precision of 0.01 g.
Width, height and the wetting angle of the clad, as well as the depth of HAZ, were measured by Image Analysis on low magnification metallographic images.
Dilution of the clad by the substrate was measured by EDXS. Small area (10x13 μm) analyses were collected on the transversal cross sections along the clad thickness, from the interface up to the external surface. Since EDXS analysis is not appropriate to get a quantitative measure of carbon content, dilution was investigated by considering iron contamination only.

RESULTS AND DISCUSSION

The energy delivered by the laser E_{TOT} is given by equation (1)

$$E_{TOT} = \frac{P \cdot l}{v} \tag{1}$$

where l is the length of the clad (80 mm).
The energy used to form the clad is given by the sum of the energy used to melt and superheat the powder E_p and the energy used to melt and superheat the substrate E_s. They are given by equations (2) and (3), respectively

$$E_p = m_p \cdot (C_{p,P}(T) \cdot \Delta T + \Delta H_{m,p}) \tag{2}$$

$$E_S = m_S \cdot (c_{P,S}(T) \cdot \Delta T + \Delta H_{\alpha \to \gamma} + \Delta H_{\gamma \to \delta} + \Delta H_{m,s} \tag{3}$$

where m_p is the mass of powder actually forming the clad (given by the mass difference of the substrate before and after cladding), $c_{p,P}(T)$ is the temperature depending specific heat of AISI316L stainless steel in both solid state and liquid state, ΔT is the difference between the maximum liquid temperature and room temperature $(T_{melt} - T_{room})$, $\Delta H_{m,p}$ is the latent heat of melting of AISI316L (275 J/g), m_s is the mass of the substrate that melts, $c_{p,s}(T)$ is the temperature depending specific heat of the carbon steel, $\Delta H_{\alpha \to \gamma}$ and $\Delta H_{\gamma \to \delta}$ are the latent heat of the $\alpha \to \gamma$ and $\gamma \to \delta$ transformations (2.4 J/g e 9.4 J/g, as measured by DSC) and $\Delta H_{m,s}$ is the latent heat of melting of the carbon steel (272 J/g).
The mass of the melted substrate was calculated from the mass balance of iron through equation (4)

$$m_{Fe,clad} = m_{Fe,P} + m_{Fe,S} \tag{4}$$

where $m_{Fe,clad}$, $m_{Fe,P}$ and $m_{Fe,S}$ are the total mass of iron in the clad, in the powder entrapped by the liquid pool and in the melted substrate; the last two parameters are given by equations (5) and (6), respectively

$$m_{Fe,P} = m_P \cdot \frac{\%Fe_p}{100} \tag{5}$$

$$m_{Fe,S} = m_S \cdot \frac{\%Fe_S}{100} \tag{6}$$

where $\%Fe_P$ and $\%Fe_S$ are the iron concentration in stainless steel (65.4%) and in the carbon steel (97.8%), respectively. Energy used to form HAZ is given by equation (7)

$$E_{HAZ} = l \cdot A_{HAZ} \cdot \rho_{subs} \cdot (C_{p,subs}(T) \cdot \Delta T' + \Delta H_{\alpha \to \gamma}) \tag{7}$$
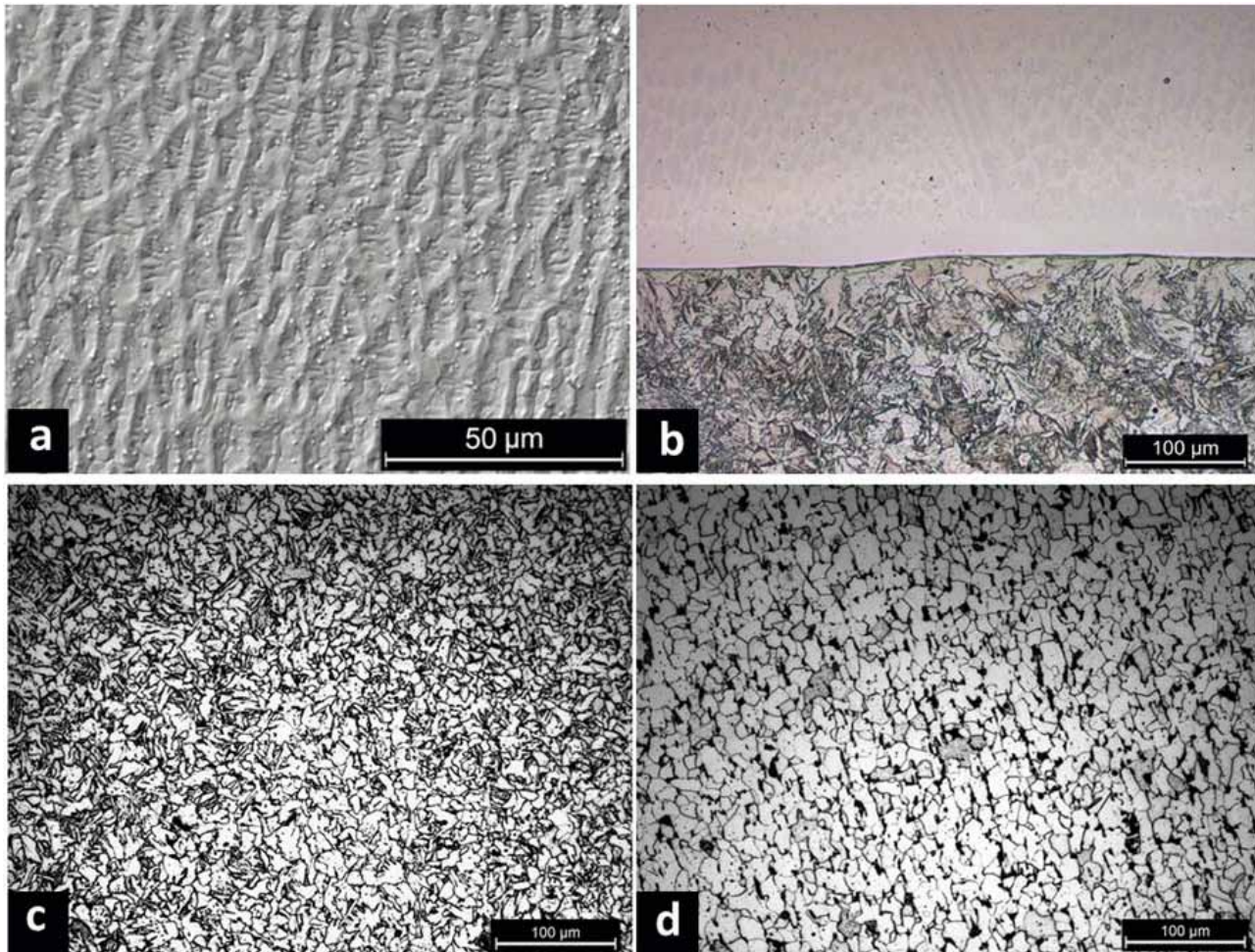
Fig. 2 - Cellular solidification structure of the clad (2a), microstructure at the interface (2b) and coarse bainitic (close to interface) and pearlitic/ferritic microstructure (close to unaffected substrate) HAZ (2c and 2d) in clad 3.

Fig. 2 - Struttura di solidificazione cellulare del cordone (2a), microstruttura all'interfaccia (2b) e microstruttura bainitica (vicino all'interfaccia, ZTA) e perlitico/ferritica (vicino al substrato non alterato termicamente) del substrato (2c e 2d) nel cordone 3.

where A_{HAZ} is the cross sectional area of HAZ, ρ_{subs} is the substrate density (7.87 g/cm³), $\Delta T' = T_{ZTA} - T_{room}$ (1173°C), $\Delta H_{\alpha \to \gamma}$ is the enthalpy of the alpha-to-gamma transformation, $c_{p,subs}(T)$ is the specific heat of the substrate. For the calculation of $\Delta T'$, T_{ZTA} was assumed as the average temperature between T_{A3} of the carbon steel and its melting temperature.

The total mass of iron in the clad was measured by EDXS. An example of the EDXS iron concentration profile in the clads is reported in Figure 3a, relevant to clad 4; the horizontal line at 65.4% Fe represents the iron concentration of the starting powder.

The iron concentration in clad 4 is higher than that of the starting powder along the whole of its thickness, with a sharp gradient in the first 100 μm from 82% down to a plateau at 68-69%. The gradient is a common feature of all the other clads, as shown by the other graphs in Figure 3, and demonstrates that even in presence of convective motions within the liquid pool a homogeneous distribution of iron is not attained. The iron concentration profiles of all the clads are reported in Figures 3b-d, grouped to highlight the effect of the heat input (clads 5, 2 and 6) and of the powder density (clads 4, 1 and 5, and clads 2 and 3). Only the gradient zone of the profiles are reported; over the thickness reported in the x axis the iron concentration is constant.

While the increase in heat input increases the iron contamination of the clad (Fig. 3b), the effect of powder density depends on heat input: at 500 J/mm (Fig. 3c) an increase in powder density leads to an attenuation of dilution; at 750 J/mm (Fig. 3d) dilution is almost unaffected.

The most diluted clads are those with either the highest heat input (6) or the lowest powder density (1 and 4), where contamination involves the whole of the thickness. Due to the inhomogeneous iron concentration, its total mass in the clads $m_{Fe,clad}$ was introduced in eq. (4) as the averaged mean value.

The cross sectional area of HAZ A_{HAZ} in eq. (7) was measured by Image analysis on the Nital etched metallographic sections.

Figure 4 shows E_p, E_s, E_{HAZ} and their sum E_{eff} versus heat
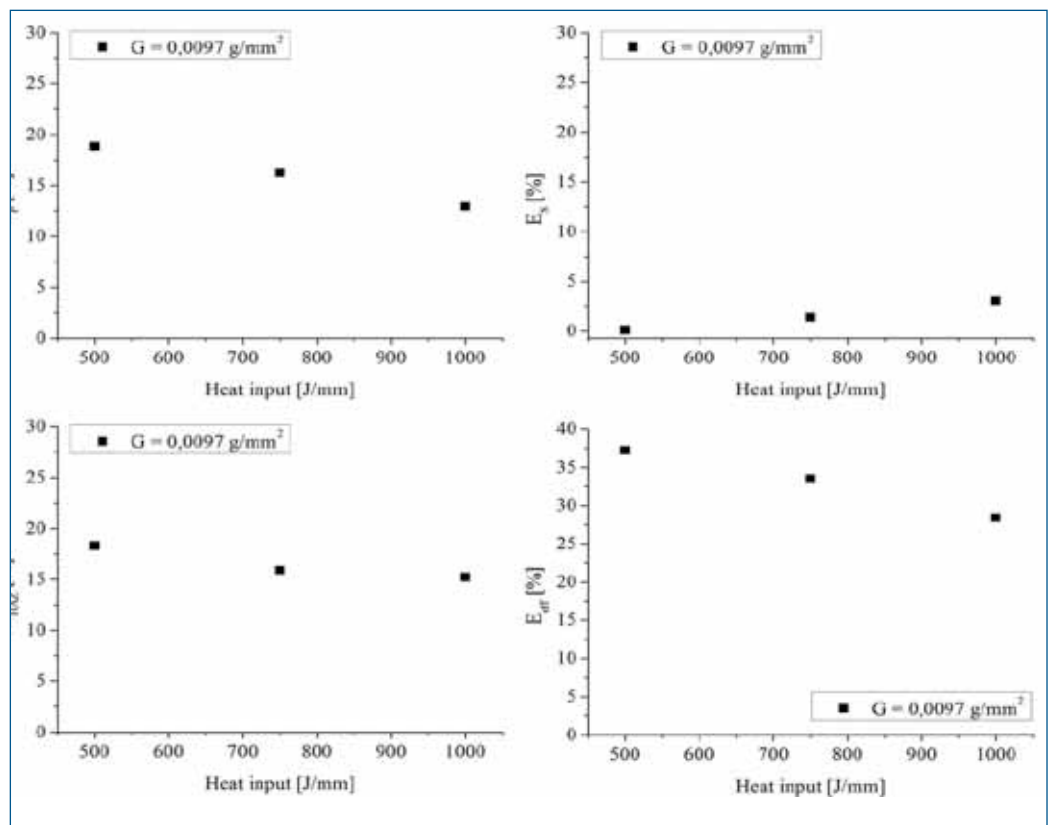
Fig. 3 - EDXS iron line profile in clad 4 (a) and in the other clads as a function of heat input (b) and of powder density (c and d).

Fig. 3 - Profilo EDXS del ferro nel cordone 4 (a) e negli altri cordoni in funzione dell'apporto di calore (b) e della densità di polvere (c e d).
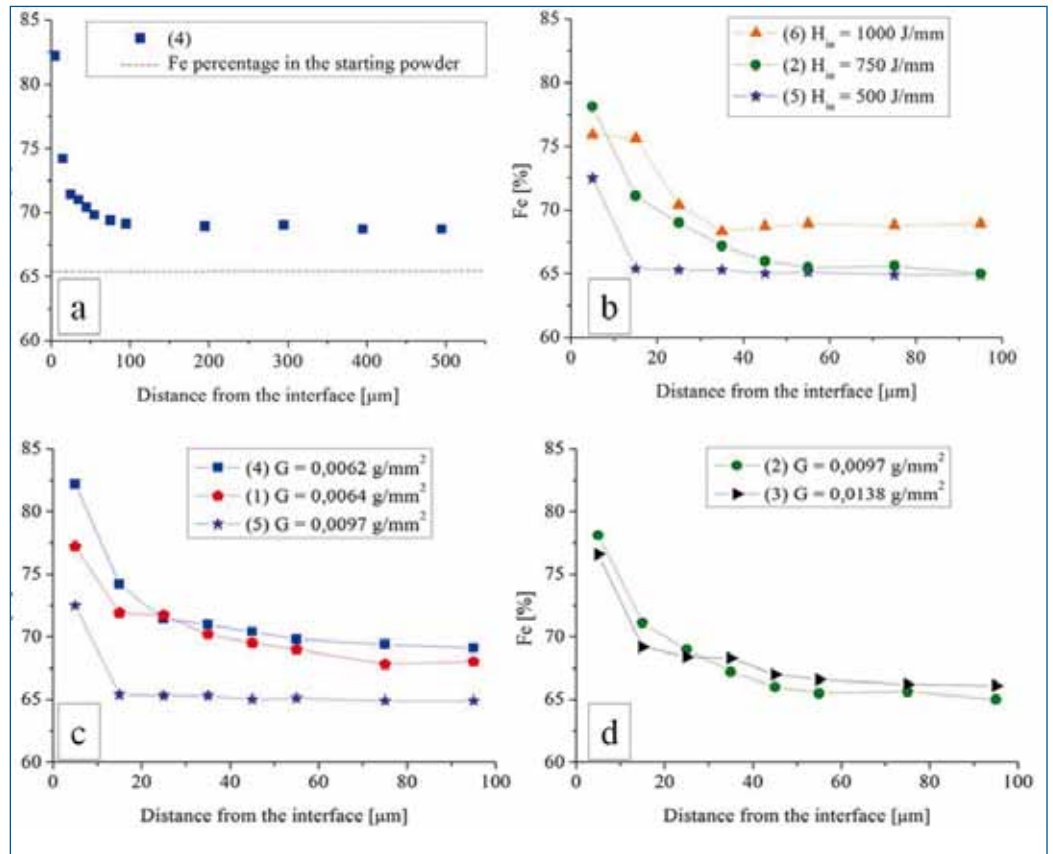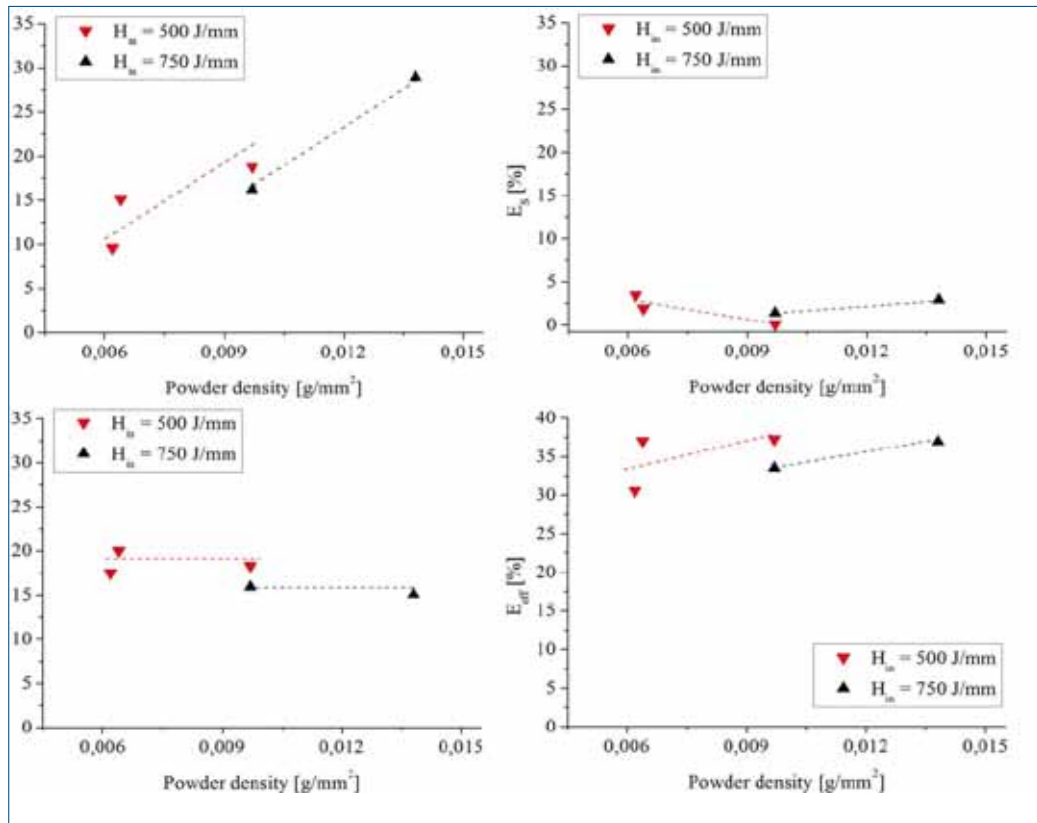

Fig. 4 - E_p, E_s, E_{HAZ} and their sum E_{eff} versus heat input at constant powder density

Fig. 4: E_p, E_s, E_{HAZ} e la loro somma E_{eff} in funzione dell'apporto di calore con densità di polvere costante
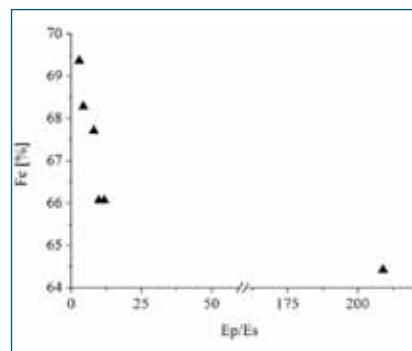
input at constant powder density.

The hypothesis of a melt temperature of 2000°C was made [5,8], since such a temperature could not be measured during the production of the clads due to technical limitations of the experimental apparatus. The energetic efficiency of the process decreases on increasing heat input, from 37.2% to 28.4% of the total energy; the remaining energy is dissipated by the following phenomena: reflection by the powder particles, radiation losses, convection losses, pull-off of hot particles from the clad zone, heating up of the plate outside the HAZ. Most of E_{eff} is spent into the powder and the HAZ (the two contributions are comparable) and only a very small percentage is utilized to melt the substrate. However, this last contribution is the one which increases with heat input, resulting in the increased dilution discussed above. Figure 5 shows E_p, E_s, E_{HAZ} and their sum E_{eff} versus powder density at constant heat input.

The efficiency of the process tends to increase with the powder density at constant heat input. This is due to the contribution of the energy spent to melt and superheat the powder entrapped into the clad, which increases with powder density. The other two terms are practically unaffected by the powder density.

The combination of a high powder density and a low heat input results in the highest energetic efficiency. This conclusion has to be verified through a further investigation by varying processing parameters systematically. Nevertheless it's interesting to observe that such a combination of powder density and heat input tends to reduce dilution of the clad. Figure 6 shows that dilution decreases on increasing the ratio between E_p and

E_s. Since E_{eff} is observed to increase with E_p and E_s has a minor effect, it may be concluded that the processing conditions that improve the energetic efficiency tend to reduce dilution of the clad.

An important characteristic of the clads is aspect ratio, defined as the ratio between width and height. A minimum aspect ratio around 5 is reported in literature [15] to avoid the formation of pores in large surface area coatings produced by multi-tracks cladding. Figure 7 shows aspect ratio versus heat input at constant powder density and versus powder density at constant heat input.
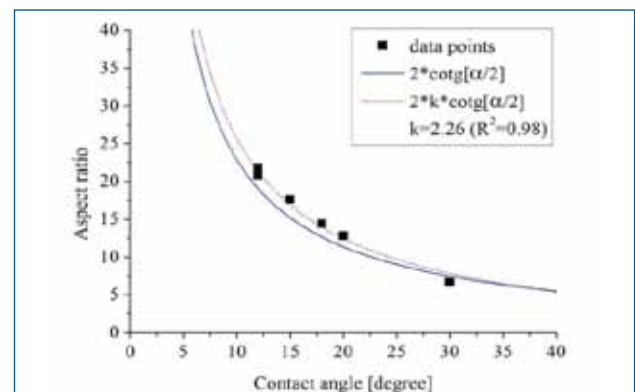
Aspect ratio increases with heat input and decreases with powder density, due to the effect of the two variables on wettability of the solid substrate by the liquid, that increases on increasing the liquid temperature [16]. Such a temperature increases on increasing heat input and on decreasing powder density since, in the latter case, a higher amount of powder is entrapped in the liquid pool. The increase in wettability increases aspect ratio, as shown in Figure 8.
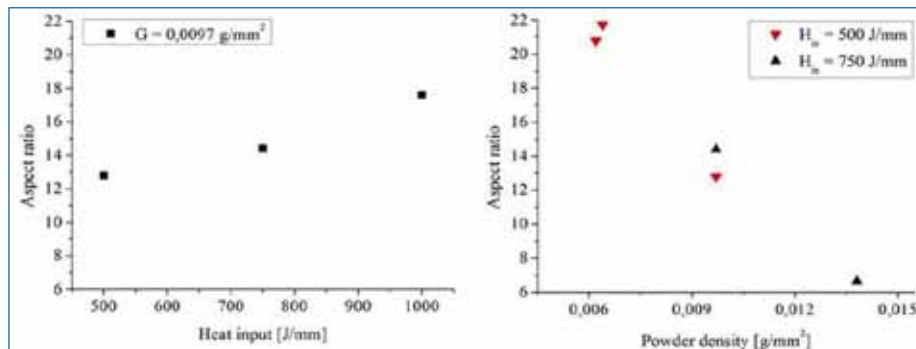
Fig. 7 - Aspect ratio versus heat input at constant powder density and versus powder density at constant heat input.

Fig. 7 - Aspect ratio in funzione dell'apporto di calore con densità di polvere costante (a) ed in funzione della densità di polvere con apporto di calore costante (b).

A simple method to correlate the aspect ratio and the contact angle is the so called $\vartheta/2$ method, which is used to measure the contact angle of a sessile drop assumed as a part of a sphere. If the part of the cross sectional area of the clads emerging from the original surface of the plate is assumed to have a spherical profile, the contact angle α can be related to the height h and the width w of the clad by the simple geometric relationship $w/h=2\cdot cot(\alpha/2)$ [9]. This equation is represented in Figure 8 by a continuous curve. The match with the experimental points is acceptable, but it is even better if a correction factor k is introduced in the above equation to account for the deviation from the spherical profile. When the correction factor k is equal to 2.26 the model gives the best result in terms of regression coefficient (R^2=0.98).

CONCLUSIONS

The results of a preliminary study of coaxial high power diode laser cladding of a carbon steel with AISI 316L powders were presented. Laser power, scan speed and feed rate were varied to obtain different values of heat input and powder density. All the clads produced are pores and crack free. The aspect ratio of the clad increases on increasing heat input and decreases on increasing powder density. This result is correlated to the temperature of the liquid pool which influences the wettability of the solid substrate by the liquid.

The energetic efficiency E_{eff}, calculated as the energy spent to form the clad and the heat affected zone, was evaluated. E_{eff} is mostly spent into the powder and the HAZ, while the contribution of the energy spent to heat up, to melt and to superheat the substrate is low.

Energetic efficiency of the process tends to increase with the powder density, while it decreases on increasing heat input. The combination of a high powder density and a low heat input is expected to optimize the energetic efficiency. In these conditions, the chemical dilution of the clad is minimized whilst aspect ratio is rather low, but still higher than the minimum value indicated in literature as safe to obtain defect-free clads. Work is in progress to investigate the geometrical and chemical characteristics of the clads and the energetic efficiency of the process by varying the process parameters systematically within broader ranges.

Fig. 8 - Aspect ratio as a function of the contact angle

Fig. 8 - Aspect ratio in funzione dell'angolo di contatto

REFERENCES

1] E. Toyserkani, A. Khajepour, S. Corbin, Laser cladding, first ed., CRC Press, Boca Raton, 2005.
2] J. Tuominen, Engineering coatings by laser cladding – the study of wear and corrosion properties, Doctoral Thesis, Tampere University of Technology, Tampere, 2009.
3] U. de Oliveira, V. Ocelík, J.Th.M. De Hosson, Surface and Coatings Technology 197 (2005) 127-136.
4] B.C. Oberlander, E. Lugscheider, Materials Science and Technology Vol. 8 (August 1992) 657-665.
5] M. Schneider, Laser cladding with powder – effect of some machining parameters on clad properties, Doctoral Thesis, University of Twente, Twente, 1998.
6] B. Ollier, N. Pirch, E. W. Kreutz, Laser und Optoelektronik 27 (1995) 1, 63-70.
7] J.M. Pelletier, M.C. Sahour, M. Pilloz, A.B. Vannes, Journal of Material Science 28 (1993) 5184-5188.
8] H. Gedda, J. Powell, G. Wahlström, W.-B. Li, H. Engström, C. Magnusson, Journal of Laser Applications Vol. 14 No. 2 (May 2002) 78-82.
9] M. Picasso, C.F. Marsden, J.-D. Wagniere, A. Frenk, M. Rappaz, Metallurgical and Materials Transactions 25B (1994) 281-291.
10] P. Vuoristo, J. Tuominen, J. Nurminen, Thermal spraying connects: explore its surfacing potential, Conference abstracts, Basel, 2005, 1270-1277.
11] A.J. Pinkerton, L. Li, Proceedings of the Institution of Mechanical Engineers, Part B: Journal of Engineering Manufacture (April 1, 2004) Vol. 218 No. 4, 363-374.
12] A.-M. El-Batahgy, Materials Letters 32 (August 1997) 155-163.
13] X. Wu, B. Zhu, X. Zeng, X. Hu, K. Cui, Surface and Coatings Technology 79 (1996) 200-204.
14] V. Ocelík, U. de Oliveira, M. de Boer, J.Th.M. de Hosson, Surface and Coatings Technology 201 (2007) 5875-5883.
15] W.M. Steen, J. Mazumder, Laser material processing, fourth ed., Springer-Verlag London Limited, 2010.
16] Y. Su, Z. Li, K.C. Mills, Journal of Material Science 40 (2005) 2201-2205.

Effetto dell'apporto di calore e della densità di polvere sull'efficienza energetica del processo di laser cladding di polvere di acciaio inossidabile AISI316L su acciaio al carbonio effettuato tramite un laser a diodi ad alta potenza

Parole chiave: Acc. inox - Rivestimenti

Un laser a diodi ad alta potenza con iniezione coassiale della polvere è stato utilizzato per depositare dei singoli cordoni di acciaio inossidabile austenitico su di un acciaio al carbonio, ed è stato studiato l'effetto dell'apporto di calore e della densità di polvere sull'efficienza energetica del processo, così come su alcune caratteristiche geometriche del cordone e sulla diluizione. L'efficienza energetica, calcolata come l'energia utilizzata per formare il cordone e la Zona Termicamente Alterata, tende ad aumentare con l'aumento della densità di polvere, mentre decresce all'aumentare dell'apporto energetico. La combinazione di un'alta densità di polvere e di un basso apporto di calore ottimizzano l'efficienza energetica del processo. In queste condizioni, la diluizione del cordone viene minimizzata mentre il valore dell'aspect ratio è piuttosto basso, seppur superiore al minimo valore accettabile.
Inoltre, l'energia spesa per le polveri e per il substrato può essere correlata con la contaminazione del rivestimento da parte del ferro del substrato.